

# Bioactive glass coatings with hydroxyapatite and Bioglass® particles on Ti-based implants. 1. Processing<sup>☆</sup>

J.M. Gomez-Vega<sup>a</sup>, E. Saiz<sup>a</sup>, A.P. Tomsia<sup>a,\*</sup>, G.W. Marshall<sup>b</sup>, S.J. Marshall<sup>b</sup>

<sup>a</sup>Materials Sciences Division, Lawrence Berkeley National Laboratory, 1 Cyclotron Road, MS 62-203, Berkeley, CA 94720, USA

<sup>b</sup>University of California, Department of Restorative Dentistry, 707 Parnassus Ave, D-2246, San Francisco, CA 94143, USA

Received 23 April 1999; accepted 28 June 1999

---

## Abstract

Silicate-based glasses with thermal expansion coefficients that match those of Ti6Al4V were prepared and used to coat Ti6Al4V by a simple enameling technique. Bioglass® (BG) or hydroxyapatite (HA) particles were embedded on the coatings in order to enhance their bioactivity. HA particles were immersed partially during heating and remained firmly embedded on the coating after cooling. There was no apparent reaction at the glass/HA interface at the temperatures used in this work (800–840°C). In contrast, BG particles softened and some infiltration into the glass coating took place during heat treatment. In this case, particles with sizes over 45 µm were required, otherwise the particles became hollow due to the infiltration and crystallization of the glass surface. The concentration of the particles on the coating was limited to 20% of surface coverage. Concentrations above this value resulted in cracked coatings due to excessive induced stress. Cracks did not propagate along the interfaces when coatings were subjected to Vickers indentation tests, indicating that the particle/glass and glass/metal interfaces exhibited strong bonds. Enameling, producing excellent glass/metal adhesion with well-attached bioactive particles on the surface, is a promising method of forming reliable and lasting implants which can endure substantial chemical and mechanical stresses. © 1999 Elsevier Science Ltd. All rights reserved.

**Keywords:** Glass coating; Enameling; Ti6Al4V; Hydroxyapatite; Bioglass®; Bioactivity

---

## 1. Introduction

Although biocompatible metallic implants are strong, their bonding ability to bone tissue is very low (bioinert materials) [1], so coatings have drawn attention as a method to improve their adherence. Various techniques have been used for coating metals with hydroxyapatite, with plasma spraying being the most common [2]. Hydroxyapatite (HA) coatings are commonly applied by plasma spray but their final composition is a mixture of amorphous and crystalline phases, leaving the coating with reduced and poorly controlled stability [3–7]. Bioglass® (BG) coatings by plasma spray usually fail due to a weak glass/metal interface and rapid dissolution in body fluids when implanted [1]. Previous attempts to coat metals with BG by an enameling technique failed

because the glass crystallized significantly, resulting in lack of adhesion to the substrate [8,9].

In previous work, glasses in the system Si–Ca–Mg–Na–K–P–O were successfully applied on Ti6Al4V using a conventional enameling technique [8]. Some of these glasses were able to form apatite *in vitro*. This work explored methods to embed BG and HA particles on the glass coating surfaces in order to improve their bioactivity, while at the same time, maintaining good adhesion to the substrate. The metal used in this work was Ti6Al4V, which is especially appropriate for implants under high stress, such as hip implants [3]. The glasses, 6P57 and 6P68, have been synthesized to match the thermal expansion coefficient of the metal, and can be used to enamel the Ti alloy.

## 2. Experimental methods

The compositions of the 6P57 and 6P68 glasses were tailored to obtain thermal expansion coefficients close to that of Ti6Al4V ( $9.6 \times 10^{-6} \text{ }^{\circ}\text{C}^{-1}$ ), as well as adequate

---

\*Corresponding author. Tel.: + 1-510-486-4918; fax: + 1-510-486-4761.

E-mail address: aptomsia@lbl.gov (A.P. Tomsia)

<sup>☆</sup>Work supported by NIH/NIDCR Grant 1R01DE11289.

Table 1  
Composition and main properties of glasses and HA

	Composition (wt%)						$\alpha$ ( $10^{-6} \text{ }^{\circ}\text{C}^{-1}$ )	$T_s$ ( $^{\circ}\text{C}$ )	E (GPa)
	SiO <sub>2</sub>	Na <sub>2</sub> O	K <sub>2</sub> O	CaO	MgO	P <sub>2</sub> O <sub>5</sub>			
6P57	56.5	11.0	3.0	15.0	8.5	6.0	10.8	609	80–90
6P68	67.7	8.3	2.2	10.1	5.7	6.0	8.8	644	80–90
BG	45.0	24.5	0.0	24.5	0.0	6.0	15.1	557	70
HA <sup>a</sup>							~14.0		110

Note:  $\alpha$  = Coefficient of thermal expansion (measured between 200 and 400°C).  
 $T_s$  = Softening point.  
E = Young's modulus.  
<sup>a</sup>HA = Ca<sub>10</sub>(PO<sub>4</sub>)<sub>6</sub>(OH)<sub>2</sub> is a double salt of tricalcium phosphate and calcium hydroxide.

Table 2  
Experimental variables studied in this work

Experimental variables	
Glass coating	6P57, 6P68
Particles	BG, HA
Particle size (μm)	(10–45), (50–100), (100–150)
Surface coverage (%)	10–80
Firing schedule	Single, double

softening points for enameling below the  $\alpha \rightarrow \beta$  transformation of Ti in the alloy ( $\sim 980^{\circ}\text{C}$ ). The glasses were prepared by mixing and firing the required reagents using a standard procedure [8]. The composition and main thermal properties of the glasses and particles used in this work are listed in Table 1. Ti6Al4V (99% purity) plates ( $15 \times 10 \times 1 \text{ mm}$ ) were ground with silicon carbide paper (800 grit) and cleaned with acetone and ethanol before their use. To manufacture the coatings, a suspension of glass powder (particle size  $< 20 \text{ }\mu\text{m}$ ) in ethanol was poured onto the plates placed in a beaker and, once the glass powder was totally settled, a second suspension of HA (99% purity) or BG particles with different sizes and concentrations was added (Table 2). The suspension of particles was dispersed using ultrasounds in order to achieve a uniform distribution of particles on the coating surface. Afterwards, the liquid was removed with a pipette and the beaker was placed in an oven at  $75^{\circ}\text{C}$  overnight to dry the green-coatings completely. The green-coatings prepared as indicated were fired in air in a Unitek dental furnace (furnace preheating to  $600^{\circ}\text{C}$ , temperature ramp  $40^{\circ}\text{C min}^{-1}$  in low vacuum, final temperature  $800^{\circ}\text{C}$ , dwell time 30 s, and quenching), as previously determined to be the optimum [10]. The final coating thickness was  $\sim 50 \text{ }\mu\text{m}$ . Particles were also deposited on coatings that were already fired. In this case, a second firing treatment in the temperature range  $720\text{--}800^{\circ}\text{C}$  was used to promote particle adhesion. The different processing variables studied in this work are summarized in Table 2.

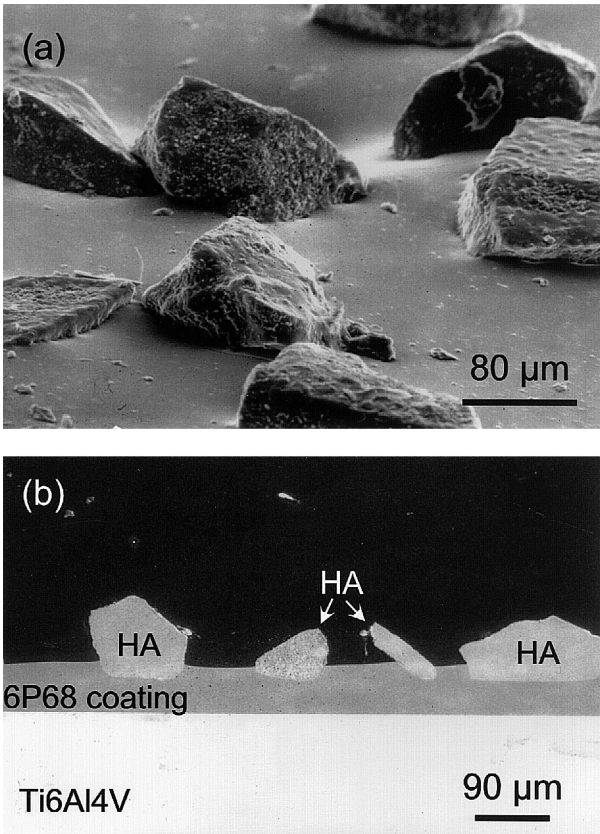


Fig. 1. Surface (a) and cross section (b) of a glass 6P68 coating with embedded HA particles (100–150  $\mu\text{m}$  diameter) fabricated by single firing.

The coating surfaces and polished cross sections were examined by optical and scanning electron microscopy with associated energy dispersive spectroscopy analysis (SEM-EDS). The percentage of the area covered by the particles was measured using image analysis of SEM and optical micrographs of the coating surface. The crystallization of the coatings was evaluated by X-ray diffraction (XRD). Phases were identified by matching the peaks to the JCPDS files. Vickers indentations (2 N load) in air

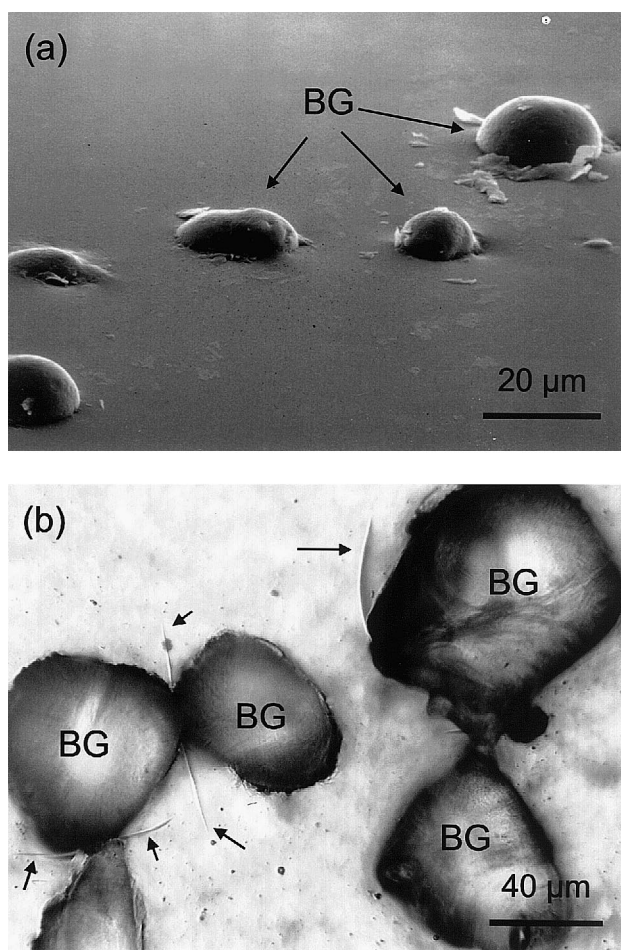


Fig. 2. Glass 6P57 coating with BG particles (10–45  $\mu\text{m}$  diameter), in (a) the particles well dispersed, whereas in (b) they are too close, resulting in cracking of the coating.

and under simulated body fluid were used to qualitatively assess the relative strengths of particle/glass and glass/metal interfaces on the coating cross sections.

### 3. Results

The surface appearance and cross section of the 6P68 glass coating with HA particles (100–150  $\mu\text{m}$ ) are shown in Fig. 1. Cracks were consistently observed in the coating when the interparticle spacing was smaller than the particle diameter. For instance, Fig. 2 shows two coatings, one with well dispersed BG particles that resulted in no cracking, and one which cracked due to small interparticle spacing. The coatings always cracked when the area fraction of particles exceeded 20%.

Fig. 3 shows the X-ray diffraction patterns taken from the glass coating surfaces. For the coatings with BG particles, sodium calcium silicate ( $\text{Na}_2\text{Ca}_2\text{Si}_3\text{O}_9$ ) crystallized on the surfaces of the coatings. As expected, hydroxyapatite was detected in the patterns of the coat-

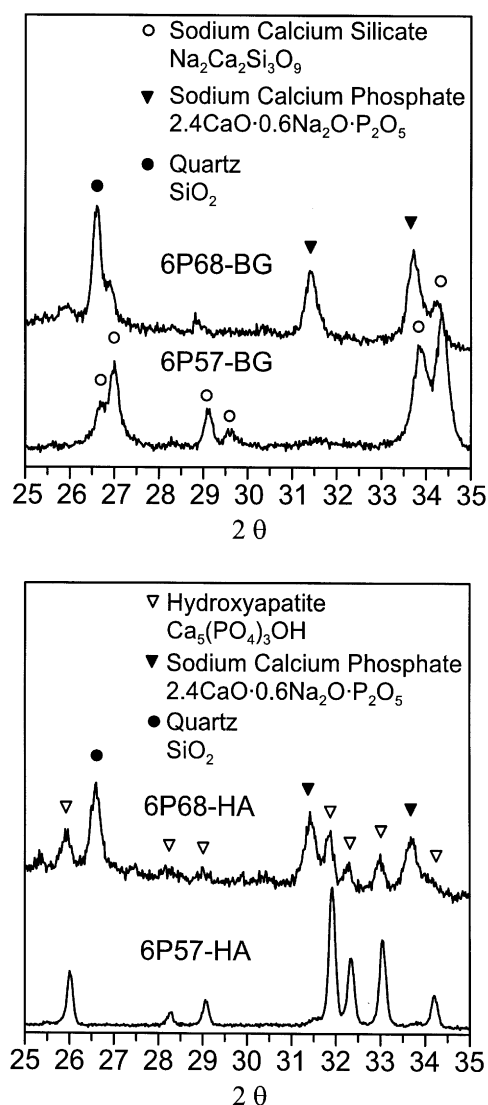


Fig. 3. XRD patterns of glass coatings with BG and HA embedded particles.

ings with embedded HA particles. Quartz and sodium calcium phosphate ( $2.4\text{CaO} \cdot 0.6\text{Na}_2\text{O} \cdot \text{P}_2\text{O}_5$ ) crystallized in the coatings fabricated with glass 6P68.

Fig. 4 shows the cross section and elemental line profile analyzed by EDS of glass 6P68 coating with BG particles embedded using a single firing procedure. Two discontinuities in the elemental concentrations were detected. In both, the concentration of  $\text{SiO}_2$ ,  $\text{MgO}$  and  $\text{K}_2\text{O}$  decreases and  $\text{CaO}$  increased towards the exterior of the coating, as expected from the corresponding glass compositions (Table 1).  $\text{P}_2\text{O}_5$  concentration remained constant at  $\sim 6$  wt%, as both glasses have the same  $\text{P}_2\text{O}_5$  content.  $\text{Na}_2\text{O}$  concentration increased gradually towards the exterior of the coating. Fig. 5 reveals that some infiltration of the BG into the glass coating at the BG/glass 6P57 interface occurred.

The behavior of the BG particles embedded in the glasses depended on their size. For the smallest particle

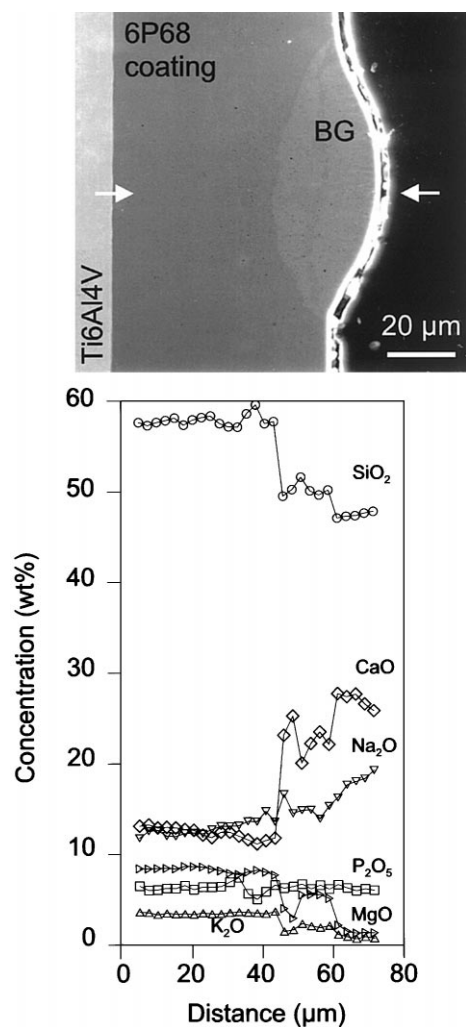


Fig. 4. Cross section and associated EDS line profile analysis for a glass 6P68 coating with an embedded BG particle.

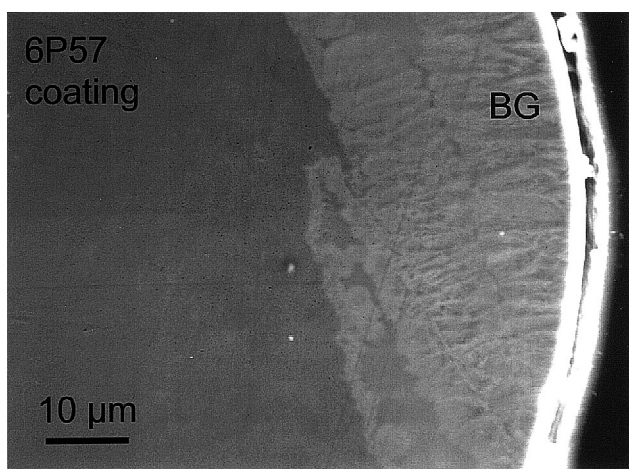


Fig. 5. SEM of the 6P57/BG interface.

size (10–45  $\mu\text{m}$ ), some particles became hollow and collapsed after firing, whereas the larger particles remained dense (Fig. 6).

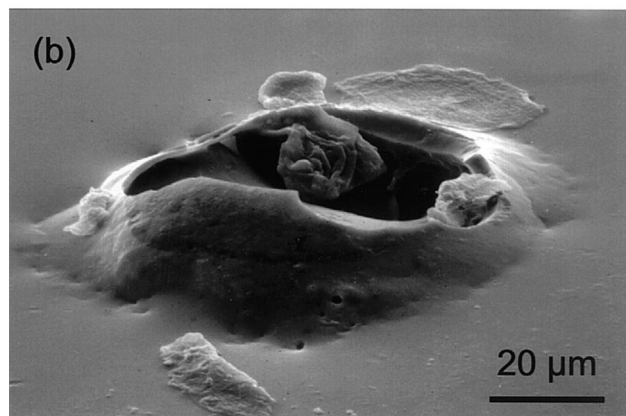
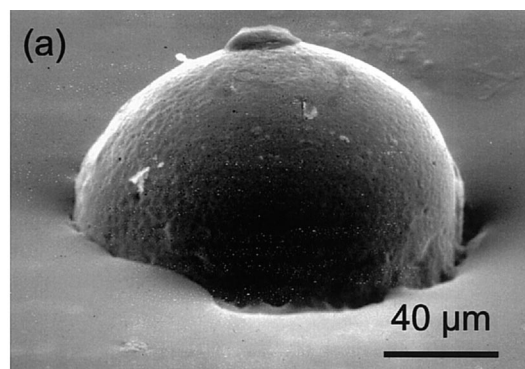


Fig. 6. SEM of BG particles with different sizes embedded in glass 6P68 (a) 50–100  $\mu\text{m}$ , (b) 10–45  $\mu\text{m}$ .

The cross sections of the coatings with HA particles showed that they are partially immersed in the glass layer after firing. EDS elemental line analysis along the HA/glass 6P57 interface revealed a single sharp transition in the concentration of all the elements at the interface (Fig. 7), in agreement with their respective compositions (Table 1).

In indentations performed on polished cross sections of these coatings, cracks did not propagate along either particle/glass or glass/metal interfaces, but rather tended to be driven into the glass coating or through the particles (Fig. 8).

#### 4. Discussion

The use of particles embedded on the surfaces of glass coatings permits novel fabrication methods that allow the introduction of materials that cannot be used directly as a coating. First, the particles induce less stress in the glass matrix than a continuous layer, and second, larger particles crystallize less than the fine powder. However, crystallization and stress generation due to thermal expansion coefficient mismatch limit the maximum concentration and size of the embedded particles.

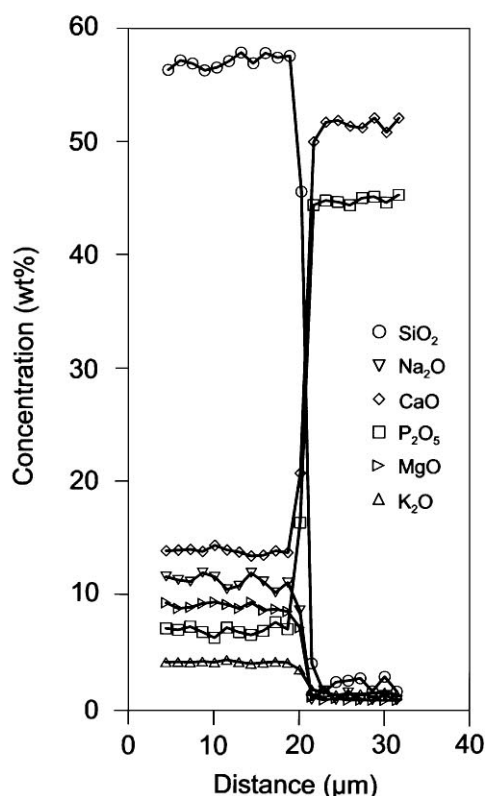
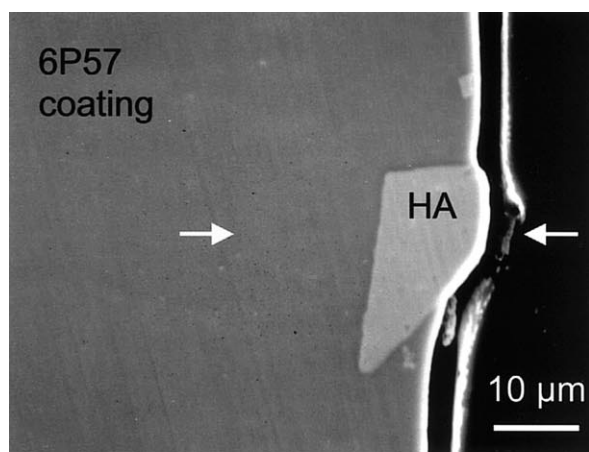


Fig. 7. Cross section and associated EDS line profile analysis for a glass 6P57 coating with an embedded HA particle.

The quantity of particles embedded in the coating is controlled by the induced stress. BG and HA particles generate stresses around them because they have higher thermal expansion than the glasses (Table 1). When the particles are too close, the thermal stresses around each particle combine and result in crazed coating matrices. For example, Fig. 9 presents the calculated radial and tangential stresses that develop during fabrication around a spherical particle of HA ( $d = 20 \mu\text{m}$ ) embedded in glass 6P57. The calculation has been performed using the elastic analysis of Selsing [11] and the values of Young's modulus, thermal expansion and glass softening

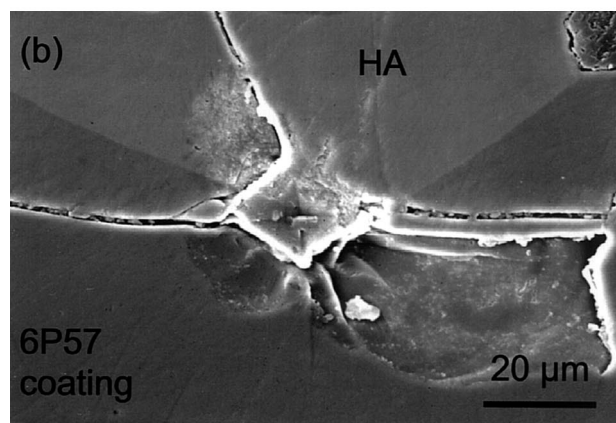
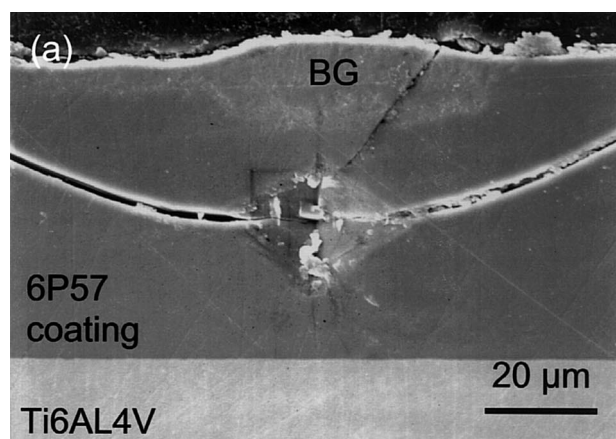


Fig. 8. Vickers indentations (0.2 kg) on cross sections of 6P57 coatings with embedded BG (a) and HA (b) particles. The cracks propagated along the glass or the particles and the interfaces did not delaminate.

point presented in Table 1. The stresses around the particle decrease exponentially with distance, becoming negligible at distances from the interface larger than the particle diameter ( $d$ ). It has been observed that coatings do not crack when the distance between particles is  $\geq d$ . The maximum surface coverage that can be obtained with circles separated by distance  $d$  is 20%, in agreement with the experimental observation that coatings were cracked when the particles covered more than 20% of the surface, or particle-particle distances were lower than  $d$ .

The qualitative evaluation of adhesion using Vickers indentation in air and under SBF indicated that glass/Ti6Al4V and glass/HA interfaces were strong. The cracks produced during the indentation never propagated along the interfaces but tended to be driven into the glass or across the particles. Indentation cracks are routinely used to study adhesion of coatings [12]. Provided that the interfacial bonding is weaker than the intrinsic bonding of the adjoining materials, the crack path will follow the interface. However, if the bonding of the interface is as strong as the cohesive bonding of both materials, there would be no preference for a crack to

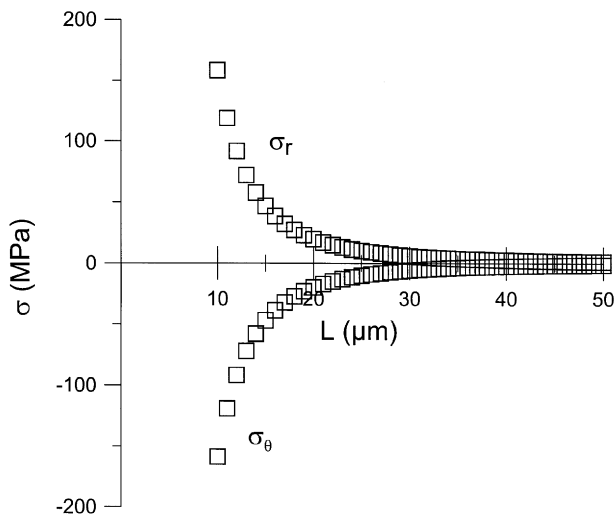


Fig. 9. Theoretical radial ( $\sigma_r$ ) and tangential ( $\sigma_\theta$ ) tensions in glass 6P57 surrounding a completely embedded spherical HA particle ( $d = 20 \mu\text{m}$ ), versus distance from its center ( $L$ ).

follow that plane exactly and some deviation would be expected. Using this method, the adhesion between the different phases can be assessed qualitatively. However, it is recognized that, due to the complex loading situations involved, in order to predict the *in vivo* response of the interfaces, a more exhaustive characterization is needed.

During firing, the glass powder flowed, wetted and coated the metal substrate while BG and HA particles behaved differently. HA particles did not melt but only immersed partially into the glass when it softened, maintaining their shape and remaining attached to the glass coating after cooling. The elemental line profile of the glass/HA interface did not show any reaction product of interdiffusion at the temperatures used in this work. This is in agreement with a previous work by Tomsia et al. where no reaction between HA and a similar silicate glass was observed at temperatures below  $850^\circ\text{C}$  [13]. Consequently, there were no significant differences in the behavior of 6P57 or 6P68 coatings with embedded HA particles.

Bioglass softening temperature is lower than that of 6P57 and 6P68 glasses (Table 1). Therefore, during firing the BG particles became rounded and some infiltration of liquid bioglass into the porous glass matrix occurred. Sodium calcium silicate crystallized on the surfaces of BG particles during the firing treatment, encapsulating the particle [8]. When the particles were too small, they were completely incorporated into the glass coating, leaving behind the crystallized crust. For the bigger particles, the firing time was too short to completely interact. More hollow BG particles were observed when glass 6P68 was used instead of 6P57, due to the higher firing temperature ( $40^\circ\text{C}$ ), which caused more crystallization and interaction. These problems may be avoided by

applying the particles to an already fired coating and using a second heat treatment at temperatures  $<800^\circ\text{C}$  to promote particle adhesion. In this case, infiltration from BG was eliminated because the particles flowed on an already dense coating. However, the adhesion of the particles to the glass was weaker and they easily detached after cooling. Similar results were obtained when the same double firing approach was used with HA particles. The adhesion of the particles to the glass 6P68 was much weaker than for 6P57 due to its higher softening point (Table 1). An additional disadvantage of the double firing is that some metal oxidation at the periphery of the coating occurred during the second heat treatment [10]. Thus, a single firing is preferred as oxidation is prevented, and better attachment of the particles is attained.

Three distinct regions were observed in the cross sections of BG containing coatings fabricated by a single firing. The inner region corresponded to the original glass coating, followed by an intermediate zone created by infiltrated bioglass, and finally the remaining BG particle which was partially crystallized.

The sodium line profile along the cross sections of glasses with embedded BG particles differed from the rest of the elements. It decreased steadily towards the interior of the coating, indicating that diffusion of Na occurred from the BG to the glass matrix. This could be expected because the diffusion coefficient of sodium in silicate glasses is much higher than for other glass elements [14].

The second part of this work will describe in detail the *in vitro* behavior of the coatings with embedded particles [15]. It has been found that apatite formed on the coating surface after one month immersion in simulated body fluid. The particles act as nucleation centers for the precipitation of apatite.

## 5. Conclusions

A simple enameling technique was used to develop durable silicate glass coatings on Ti6Al4V substrates. HA and/or BG particles were incorporated into these coatings to promote increased bioactivity. The effectiveness of BG incorporation depended on the softening temperature of the glass coating, with higher softening temperatures leading to increased degradation of the BG. This was not the case for HA. Incorporation of  $\sim 20\%$  of either particle type was successfully accomplished without cracking or loss of adhesion to the melted substrate, in agreement with theoretical predictions.

## Acknowledgements

This work was supported by NIH/NIDCR Grant 1R01DE11289. Jose M. Gomez-Vega wishes to thank FICYT for the postdoctoral fellowship given to him in

the II Plan Regional de Investigación del Principado de Asturias (Spain).

## References

- [1] Hench LL, Andersson Ö. Bioactive glass coatings. In: Hench LL, Wilson J, editors. *An introduction to bioceramics*. Singapore: World Scientific, 1993. p. 239–59.
- [2] Kitsugi T, Nakamura T, Oka M, Senaha Y, Goto T, Shibuya T. Bone-bonding behavior of plasma-sprayed coatings of Bioglass®, AW-glass ceramic, and tricalcium phosphate on titanium alloy. *J Biomed Mater Res* 1996;30:261–9.
- [3] Hench LL. Bioceramics: from concept to clinic. *J Am Ceram Soc* 1991;74:1487–510.
- [4] Suchanek W, Yoshimura M. Processing and properties of hydroxyapatite-based biomaterials for use as hard tissue replacement implants. *J Mater Res* 1998;13:94–117.
- [5] Lacefield WR. Hydroxylapatite coating. In: Hench LL, Wilson J, editors. *An introduction to bioceramics*. Singapore: World Scientific, 1993. p. 223–38.
- [6] Ha SW, Reber R, Ecjert KL, Petitmermet M, Mayer J, Wintermanterl E, Baerlacher Ch, Gruner H. Chemical and morphological changes of vacuum-plasma-sprayed hydroxyapatite coatings during immersion in simulated physiological solutions. *J Am Ceram Soc* 1998;81:81–8.
- [7] Gross KA, Gross V, Berdin CC. Thermal analysis of amorphous phases in hydroxyapatite coatings. *J Am Ceram Soc* 1998;81:106–12.
- [8] Pazo A, Saiz E, Tomsia AP. Silicate glass coatings on Ti-based implants. *Acta Mater* 1998;46:2551–8.
- [9] Pazo A, Saiz E, Tomsia AP. Bioactive coatings on Ti and Ti6Al4V alloys for medical applications. In: Tomsia AP, Glaeser AM, editors. *Ceramic microstructures*. New York: Plenum Press, 1998. p. 543–50.
- [10] Gomez-Vega JM, Saiz E, Tomsia AP. Glass-based coatings for titanium implant alloys. *J Biomed Mater Res* 1999;46:549–59.
- [11] Selsing J. Internal stresses in ceramics. *J Am Ceram Soc* 1961;44: 419–26.
- [12] Chalker PR, Bull SJ, Rickerby DS. A review of the methods for the evaluation of coating-substrate adhesion. *Mater Sci Eng* 1991;140:583–92.
- [13] Tomsia AP, Moya JS, Guitian F. New route for hydroxyapatite coatings on Ti-based human implants. *Scripta Metall Mater* 1994;31:995–1000.
- [14] Johnson JR, Bristow RH, Blau HH. Diffusion of ions in some simple glasses. *J Am Ceram Soc* 1951;34:165–72.
- [15] Gomez-Vega JM, Saiz E, Tomsia AP, Marshall GW, Marshall SJ. Bioactive glass coatings with hydroxyapatite and Bioglass® particles on Ti-based implants. 2. In vitro behavior. *Biomaterials*, submitted for publication.